

Group Sequential Design with Posterior and Posterior Predictive Probabilities

Luke Hagar*

Shirin Golchi*

Marina B. Klein†

**Department of Epidemiology, Biostatistics & Occupational Health, McGill University*

†*McGill University Health Centre, McGill University*

Abstract

Group sequential designs drive innovation in clinical, industrial, and corporate settings. Early stopping for failure in sequential designs conserves experimental resources, whereas early stopping for success accelerates access to improved interventions. Bayesian decision procedures provide a formal and intuitive framework for early stopping using posterior and posterior predictive probabilities. Design parameters including decision thresholds and sample sizes are chosen to control the error rates associated with the sequential decision process. These choices are routinely made based on estimating the sampling distribution of posterior summaries via intensive Monte Carlo simulation for each sample size and design scenario considered. In this paper, we propose an efficient method to assess error rates and determine optimal sample sizes and decision thresholds for Bayesian group sequential designs. We prove theoretical results that enable posterior and posterior predictive probabilities to be modeled as a function of the sample size. Using these functions, we assess error rates at a range of sample sizes given simulations conducted at only two sample sizes. The effectiveness of our methodology is highlighted using two substantive examples.

Keywords: Bayesian sample size determination; clinical trials; experimental design; quality control; sequential hypothesis testing

1 Introduction

Scientific experiments drive progress across a wide range of disciplines, including medicine, manufacturing, public transportation, and consumer marketing. However, there are substantial financial and human costs associated with experimentation related to the exploration-exploitation dilemma (Berger-Tal et al., 2014). Exploring new interventions to assess their suitability is crucial to foster innovation, but ethical and economic concerns arise when accruing knowledge is not exploited to offer people the best available intervention. Superior interventions should be implemented and inferior ones should be discontinued as quickly as possible. Sequential designs (Wald, 2004) can address this exploration-exploitation dilemma and reduce the costs of experimentation. Group sequential designs divide experiments into stages, analyzing data after each stage to decide whether to continue based on predefined discontinuation rules (Bross, 1952; Jennison and Turnbull, 1999). Early stopping for success is based on evidence from the data that a new intervention is beneficial, whereas early stopping for failure is based on evidence of ineffectiveness. Competing null and alternative

*Luke Hagar is the corresponding author and may be contacted at lmhagar@uwaterloo.ca.

hypotheses – H_0 and H_1 – respectively characterize settings where a new intervention is ineffective and beneficial.

To ensure sequential designs reliably inform decision making, it is important to control the error rates associated with their decision procedures. These error rates are the probabilities of making incorrect decisions across all analyses, such as stopping for success when H_0 is true or not stopping for success under H_1 . The error rates of sequential designs are typically controlled by selecting suitable sample sizes and decision thresholds for the repeated analyses. Popular methods for selecting decision thresholds adjust for the inflated type I error risk linked to early stopping for success in group sequential designs (Pocock, 1977; O'Brien and Fleming, 1979; Demets and Lan, 1994). Decision thresholds related to early stopping for failure have historically been chosen using stochastic curtailment procedures (Halperin et al., 1982; Lachin, 2005). These procedures advocate for stopping if there is a low probability of achieving the experiment's objective in its remaining stages given the available data and assumptions about the future data. The aforementioned methods were developed with a primary focus in frequentist design of experiments.

Bayesian methods provide a formal and intuitive framework for early stopping in sequential designs based on posterior summaries. For example, the experiment can be stopped for success at any analysis if the posterior probability that H_1 is true exceeds the corresponding decision threshold. Posterior predictive probabilities (Rubin, 1984; Gelman et al., 1996; Berry et al., 2010; Saville et al., 2014) quantify the probability that the posterior probability that H_1 is true at a future analysis exceeds its decision threshold. The experiment can be stopped for success or failure depending on whether this posterior predictive probability is sufficiently large or small. Posterior predictive probabilities serve as a Bayesian analog to stochastic curtailment with fewer explicit assumptions about the future data, which are generated based on the current posterior. Even when Bayesian posterior summaries inform decision making, sample sizes and decision thresholds are often chosen to control the frequentist error rates of sequential designs. Regulatory agencies require strict control of error rates in clinical settings (FDA, 2019), but the frequentist error rates of Bayesian designs are of much broader interest (see e.g., Jenkins and Peacock (2011); Deng et al. (2024)).

Wang and Gelfand (2002) proposed a general framework to determine suitable sample sizes and decision thresholds that uses Monte Carlo simulation to estimate error rates of Bayesian designs. This computational approach estimates sampling distributions of posterior summaries by simulating many iterations of an experiment according to a particular data generation process. Gubbiotti and De Santis (2011) defined two methodologies for specifying the data generation process; the conditional approach uses fixed values for the data generating parameters and the predictive approach accommodates uncertainty in these values. With either approach, the repeated estimation of joint sampling distributions across the stages of a sequential design requires substantial computing resources. A general and efficient method for group sequential design with posterior and posterior predictive probabilities would make these designs more accessible to practitioners.

Various strategies have recently been proposed to reduce the computational overhead required to estimate sampling distributions of posterior summaries. [Golchi \(2022\)](#) and [Golchi and Willard \(2024\)](#) proposed flexible modeling approaches to estimate sampling distributions of univariate summaries. [Hagar and Stevens \(2025\)](#) developed a method to estimate the sampling distribution of posterior probabilities throughout the sample size space using estimates of the sampling distribution at only two sample sizes. Because these approaches do not consider the joint sampling distribution of posterior summaries across multiple analyses, they are not suitable for sequential designs. In this work, we build upon the method from [Hagar and Stevens \(2025\)](#) to accommodate both sequential designs and the use of posterior predictive probabilities. These useful extensions are predicated on a series of theoretical results that are original to this paper. While our framework is theoretically intricate, its implementation is straightforward, promoting an economical and broadly useful approach to simulation-based design for Bayesian sequential experiments. Our proposed methods could be applied to various types of sequential designs, but this paper focuses on group sequential designs given their prevalence in decision making.

The remainder of this article is structured as follows. In Section 2, we introduce preliminary concepts required to describe our methods. In Section 3, we construct proxies to the joint sampling distribution of posterior and posterior predictive probabilities in group sequential designs and prove novel theoretical results about these proxies. We adapt these theoretical results to develop a procedure to select sample sizes and decision thresholds that requires estimation of the true joint sampling distribution of posterior and posterior predictive probabilities at only two sample sizes in Section 4. In Section 5, we showcase the strong performance of our methodology with two examples that span clinical and industrial contexts to reflect the broad applicability of our framework for group sequential design. We conclude with a summary and discussion of extensions to this work in Section 6.

2 Preliminaries

This paper focuses on Bayesian group sequential designs in which predefined stopping rules leverage posterior and posterior predictive probabilities about the target of inference. The statistical model for the experiment is defined using a set of parameters $\boldsymbol{\theta} \in \Theta$. The target of inference is a function of these parameters: $\delta(\boldsymbol{\theta}) \in \mathbb{R}$. The interval hypotheses that inform decision making are $H_0 : \delta(\boldsymbol{\theta}) \notin (\delta_L, \delta_U)$ vs. $H_1 : \delta(\boldsymbol{\theta}) \in (\delta_L, \delta_U)$, where $-\infty \leq \delta_L < \delta_U \leq \infty$. This general notation for the interval endpoints accommodates hypothesis tests based on superiority, noninferiority, and practical equivalence. The posterior distribution of $\delta(\boldsymbol{\theta})$ synthesizes information from the prior distribution for $\boldsymbol{\theta}$ and the available data.

Sequential experiments have T potential analyses indexed by $t \in \{1, \dots, T\}$. From a design perspective, our notation treats the data from all stages of the experiment as observable since complete data for the experiment can be simulated. At the t^{th} analysis, the cumulative n_t observations comprise the data, $\mathcal{D}_{n_t} =$

$\{\mathbf{Y}_{n_t \times 1}, \mathbf{X}_{n_t \times w}\}$, consisting of outcomes $\mathbf{Y}_{n_t \times 1}$ and w additional covariates $\mathbf{X}_{n_t \times w}$ for each observation. All observations accrued in previous stages are retained in \mathcal{D}_{n_t} for subsequent analyses. Because data from all T stages will not be observed in a given experiment if the experiment stops early, we describe how our design methodology accounts for early stopping later in this section.

We flexibly accommodate sequential designs that can facilitate stopping for both success and failure based on posterior or posterior predictive probabilities. As discussed later, aspects of our general notation can be simplified for a given design. We first consider stopping rules based on posterior probabilities. Our theoretical development in Section 3 considers joint sampling distributions across all T analyses irrespective of the interim decisions. We use these *complete* sampling distributions to efficiently design group sequential experiments with interim decision rules in Section 4. We index the complete joint sampling distribution of posterior probabilities using the sample size for the first analysis. Specifically, we index by a sample size n such that $\{n_1, n_2, \dots, n_T\} = n \times \{c_1, c_2, \dots, c_T\}$ for some constants $c_1 = 1$ and $\{c_t\}_{t=2}^T > 1$. The data $\mathcal{D}_n = \{\mathcal{D}_{n_t}\}_{t=1}^T$ across all analyses define a vector of T posterior probabilities about the hypothesis H_1 :

$$\boldsymbol{\tau}(\mathcal{D}_n) = \begin{bmatrix} \tau_1(\mathcal{D}_n) \\ \vdots \\ \tau_T(\mathcal{D}_n) \end{bmatrix} = \begin{bmatrix} \Pr(H_1 \mid \mathcal{D}_{n_1}) \\ \vdots \\ \Pr(H_1 \mid \mathcal{D}_{n_T}) \end{bmatrix}. \quad (1)$$

Stopping for success may be facilitated by comparing $\boldsymbol{\tau}(\mathcal{D}_n)$ to success thresholds $\boldsymbol{\gamma} = \{\gamma_t\}_{t=1}^T \in [0, 1]^T$. If not already stopped in a previous stage, the experiment may be stopped for success at analysis t if $\tau_t(\mathcal{D}_n) \geq \gamma_t$. Stopping for failure could be facilitated by comparing $\boldsymbol{\tau}(\mathcal{D}_n)$ to failure thresholds $\boldsymbol{\xi} = \{\xi_t\}_{t=1}^T < \{\gamma_t\}_{t=1}^T$. If not previously stopped, the experiment can be stopped for failure at analysis t if $\tau_t(\mathcal{D}_n) < \xi_t$.

We next overview stopping rules based on posterior predictive probabilities. The posterior predictive distribution characterizes the distribution of future data according to the current posterior distribution (Rubin, 1984; Gelman et al., 1996). The posterior predictive distribution $p_{\mathbf{P}}(y \mid \mathcal{D}_{n_t})$ at analysis t is defined as

$$p_{\mathbf{P}}(y \mid \mathcal{D}_{n_t}) = \int_{\Theta} p(y \mid \boldsymbol{\theta}) p(\boldsymbol{\theta} \mid \mathcal{D}_{n_t}) d\boldsymbol{\theta}, \quad (2)$$

where $p(y \mid \boldsymbol{\theta})$ is the assumed model for the outcome and $p(\boldsymbol{\theta} \mid \mathcal{D}_{n_t})$ is the current posterior distribution. Posterior predictive probabilities generally represent probability statements about future data or parameters that are inferred from a posterior that incorporates these future data. Following common practice (Berry et al., 2010; Saville et al., 2014), we specifically consider the posterior predictive probability for an analysis $t < T$ as the probability that $\tau_T(\mathcal{D}_n)$ will be at least γ_T given the current data \mathcal{D}_{n_t} . This probability is considered when the data generation process for the remaining $n_T - n_t$ observations is the posterior predictive distribution in (2):

$$\Pr\{\Pr(H_1 \mid \mathcal{D}_{n_T}) \geq \gamma_T \mid \mathcal{D}_{n_t}\} = \int_{\Theta} \Pr\{\Pr(H_1 \mid \mathcal{D}_{n_T}) \geq \gamma_T \mid \boldsymbol{\theta}\} p(\boldsymbol{\theta} \mid \mathcal{D}_{n_t}) d\boldsymbol{\theta}. \quad (3)$$

The posterior predictive distribution can be obtained analytically for simple models with conjugate priors (Saville et al., 2014), but the *intensive* simulation-based procedure that follows is generally applicable. First, a sample value $\boldsymbol{\theta}^{(m)}$ is drawn from the posterior distribution $p(\boldsymbol{\theta} \mid \mathcal{D}_{n_t})$. Second, $n_T - n_t$ observations are generated from the assumed model $p(y \mid \boldsymbol{\theta}^{(m)})$ and combined with \mathcal{D}_{n_t} to create $\mathcal{D}_{n_T}^{(m)}$. Third, the posterior distribution $p(\boldsymbol{\theta} \mid \mathcal{D}_{n_T}^{(m)})$ is approximated to compute the posterior probability $\Pr(H_1 \mid \mathcal{D}_{n_T}^{(m)})$. These three steps are repeated M times. The posterior predictive probability in (3) is estimated as $M^{-1} \sum_{m=1}^M \mathbb{I}\{\Pr(H_1 \mid \mathcal{D}_{n_T}^{(m)}) \geq \gamma_T\}$.

For illustration, we suppose that the sequential design could stop based on posterior predictive probabilities at any of the first $T - 1$ analyses. The data, indexed by the sample size n for the first analysis, define a vector of $T - 1$ posterior predictive probabilities:

$$\boldsymbol{\tau}_P(\mathcal{D}_n) = \begin{bmatrix} \tau_{P,1}(\mathcal{D}_n) \\ \vdots \\ \tau_{P,T-1}(\mathcal{D}_n) \end{bmatrix} = \begin{bmatrix} \Pr\{\Pr(H_1 \mid \mathcal{D}_{n_T}) \geq \gamma_T \mid \mathcal{D}_{n_1}\} \\ \vdots \\ \Pr\{\Pr(H_1 \mid \mathcal{D}_{n_T}) \geq \gamma_T \mid \mathcal{D}_{n_{T-1}}\} \end{bmatrix}. \quad (4)$$

Early stopping for success and failure could be implemented by comparing $\boldsymbol{\tau}_P(\mathcal{D}_n)$ to success thresholds $\boldsymbol{\eta} = \{\eta_t\}_{t=1}^{T-1} \in [0, 1]^{T-1}$ and failure thresholds $\boldsymbol{\rho} = \{\rho_t\}_{t=1}^{T-1} < \{\eta_t\}_{t=1}^{T-1}$. If not stopped in a previous stage, the experiment may be respectively stopped for success or failure at analysis t if $\tau_{P,t}(\mathcal{D}_n) \geq \eta_t$ or $\tau_{P,t}(\mathcal{D}_n) < \rho_t$.

To theoretically examine error rates in sequential designs with stopping rules based on posterior predictive probabilities, we must consider the joint sampling distribution of the posterior probabilities in (1) and the posterior predictive probabilities in (4) irrespective of the interim decisions. We jointly refer to these probabilities as

$$\boldsymbol{\tau}_*(\mathcal{D}_n) = \begin{bmatrix} \boldsymbol{\tau}(\mathcal{D}_n) \\ \boldsymbol{\tau}_P(\mathcal{D}_n) \end{bmatrix}.$$

Our general notation concerns the complete joint sampling distribution of $\boldsymbol{\tau}_*(\mathcal{D}_n)$; however, any specific design may consider the subset of components in $\boldsymbol{\tau}_*(\mathcal{D}_n)$ that inform the pre-specified decision rules. To estimate the sampling distribution of $\boldsymbol{\tau}_*(\mathcal{D}_n)$ via simulation, we define various data generation processes for \mathcal{D}_n . For each Monte Carlo iteration, data are generated according to a fixed parameter value $\boldsymbol{\theta}$. The probability model Ψ characterizes how $\boldsymbol{\theta}$ values are drawn in Monte Carlo iteration $r = 1, \dots, R$. The probability model Ψ could be viewed as a *design* prior (De Santis, 2007; Gubbiotti and De Santis, 2011) that differs from the *analysis* prior $p(\boldsymbol{\theta})$. This notation accommodates the conditional and predictive approaches, where Ψ is a degenerate probability model under the conditional approach. For each iteration r , complete data $\mathcal{D}_{n,r}$ across all T stages are generated given $\boldsymbol{\theta}_r \sim \Psi$, and $\boldsymbol{\tau}_*(\mathcal{D}_{n,r})$ is computed. Across R Monte Carlo iterations, the collection of obtained $\{\boldsymbol{\tau}_*(\mathcal{D}_{n,r})\}_{r=1}^R$ values estimates the joint sampling distribution of $\boldsymbol{\tau}_*(\mathcal{D}_n)$.

To consider the error rates of sequential designs with general stopping rules, we define a binary indicator $\nu(\mathcal{D}_n)$ that equals 1 if and only if the experiment stops for *success* at any analysis $t = 1, \dots, T$. We consider

an example design with $T = 2$ analyses to underscore the relationship between $\tau_*(\mathcal{D}_n)$ and $\nu(\mathcal{D}_n)$. For illustration, this example design considers stopping for success based on $\tau(\mathcal{D}_n)$ before considering stopping for failure based on $\tau_P(\mathcal{D}_n)$. We have that $\nu(\mathcal{D}_n) = 1$ based on the first analysis if and only if $\tau_1(\mathcal{D}_n) \geq \gamma_1$. Moreover, $\nu(\mathcal{D}_n) = 1$ based on the second analysis if and only if $\tau_1(\mathcal{D}_n) < \gamma_1$, $\tau_{P,1}(\mathcal{D}_n) \geq \rho_1$, and $\tau_2(\mathcal{D}_n) \geq \gamma_2$.

We now define error rates with respect to the model from which $\boldsymbol{\theta}$ values are drawn. For a given model Ψ , the probability of stopping for success across all analyses is

$$\mathbb{E}_\Psi[\Pr(\nu(\mathcal{D}_n) = 1 \mid \boldsymbol{\theta})] = \int \Pr(\nu(\mathcal{D}_n) = 1 \mid \boldsymbol{\theta}) \Psi(\boldsymbol{\theta}) d\boldsymbol{\theta}. \quad (5)$$

Given the simulation results, the probability in (5) is estimated as

$$\frac{1}{R} \sum_{r=1}^R \mathbb{I}\{\nu(\mathcal{D}_{n,r}) = 1\}, \quad (6)$$

where $\mathcal{D}_{n,r}$ are generated using $\boldsymbol{\theta}_r$ obtained via Ψ . The type II error rate associated with incorrectly not stopping for success is $\mathbb{E}_{\Psi_1}[\Pr(\nu(\mathcal{D}_n) = 0 \mid \boldsymbol{\theta})]$ where Ψ_1 is a probability model such that H_1 is true. Power is the complementary probability $\mathbb{E}_{\Psi_1}[\Pr(\nu(\mathcal{D}_n) = 1 \mid \boldsymbol{\theta})]$, and we estimate power using (6) when $\{\mathcal{D}_{n_t,r}\}_{t=1}^T$ are generated using $\boldsymbol{\theta}_r$ obtained via Ψ_1 . The type I error rate related to incorrectly stopping for success is $\mathbb{E}_{\Psi_0}[\Pr(\nu(\mathcal{D}_n) = 1 \mid \boldsymbol{\theta})]$ where Ψ_0 is a probability model such that H_0 is true. Using Ψ_0 instead of Ψ_1 , this probability can be estimated as in (6). We note that power and the type I error rate can be computed using an estimate of the *complete* joint sampling distribution $\{\tau_*(\mathcal{D}_{n,r})\}_{r=1}^R$. In iteration r , suppose the t^{th} analysis is the first one at which $\tau_t(\mathcal{D}_{n,r})$ or $\tau_{P,t}(\mathcal{D}_{n,r})$ prompts stopping for success or failure. We can then simply ignore the rows in $\tau_*(\mathcal{D}_{n,r})$ that correspond to analyses $t+1, \dots, T$. For this reason, we theoretically consider and model complete joint sampling distributions in this paper.

The success thresholds $\boldsymbol{\gamma}$ and $\boldsymbol{\eta}$ bound the type I error rate of sequential designs. Standard methods for group sequential design (Jennison and Turnbull, 1999) prompt initial threshold values that could be tuned using Monte Carlo simulation. The sample sizes $\{n_t\}_{t=1}^T$ are selected to ensure the experiment has a small enough type II error rate (i.e., to guarantee power is sufficiently large). The failure thresholds $\boldsymbol{\xi}$ and $\boldsymbol{\rho}$ are often chosen to ensure stopping for failure does not greatly inflate the type II error rate. For every value of $n = n_1$ considered, we must obtain a collection of $\{\tau_*(\mathcal{D}_{n,r})\}_{r=1}^R$ values via simulation to estimate error rates, while tuning the decision thresholds if necessary. The process to obtain the $\{\tau_*(\mathcal{D}_{n,r})\}_{r=1}^R$ values is computationally intensive. However, we can reduce the computational burden by using previously estimated sampling distributions of $\tau_*(\mathcal{D}_n)$ to estimate error rates at new n values without conducting additional simulations. We can use this process to efficiently design Bayesian sequential experiments. We propose such a design method in this paper and begin its development in Section 3.

3 Proxies to the Joint Sampling Distribution

3.1 Proxies to Posterior Probabilities

To motivate our design procedure proposed in Section 4, we create a proxy to the joint sampling distribution of $\tau_*(\mathcal{D}_n)$ irrespective of the interim decisions. These proxies are needed for the theory that substantiates our proposed methodology. However, our methods do not directly use these proxies and instead estimate the true sampling distribution of $\tau_*(\mathcal{D}_n)$ by simulating samples $\{\mathcal{D}_{n,r}\}_{r=1}^R$ and approximating posterior summaries as described in Section 2. We create a proxy for the joint sampling distribution of posterior probabilities $\tau(\mathcal{D}_n)$ in this subsection and augment this proxy to accommodate posterior predictive probabilities in Section 3.2. Our proxies are predicated on an asymptotic approximation to the posterior of $\delta = \delta(\boldsymbol{\theta})$ based on the Bernstein-von Mises (BvM) theorem outlined in Chapter 10.2 of [van der Vaart \(1998\)](#).

The four conditions for the BvM theorem must therefore be satisfied to apply our methodology. The first three conditions concern the likelihood function and are also required for the asymptotic normality of the maximum likelihood estimator (MLE), detailed in Theorem 5.39 of [van der Vaart \(1998\)](#). For reasons described shortly, our methodology also requires that those regularity conditions are satisfied. The final condition for the BvM theorem concerns the analysis prior $p(\boldsymbol{\theta})$. This prior must be absolutely continuous with positive density in a neighborhood of the true value for $\boldsymbol{\theta}$. This true value is $\boldsymbol{\theta}_r \sim \Psi$ in iteration r . For the r^{th} iteration, we let $\hat{\delta}_r^{(n)}$ be the maximum likelihood estimate for $\delta(\boldsymbol{\theta})$ corresponding to an analysis with n accrued observations. The limiting posterior of δ for this single analysis prompted by the BvM theorem is

$$\mathcal{N}\left(\hat{\delta}_r^{(n)}, \sigma_r^2/n\right), \quad (7)$$

where the variance σ_r^2 is related to the Fisher information $\mathcal{I}(\boldsymbol{\theta})$ evaluated at $\boldsymbol{\theta} = \boldsymbol{\theta}_r$. We only use the posterior in (7) for theoretical development and need not obtain σ_r^2 in practice.

In sequential designs, the posterior distributions of δ at distinct analyses are not independent because the data from earlier stages are retained throughout the experiment. Our proxies account for this dependence via the joint sampling distribution of the MLE $\hat{\boldsymbol{\delta}}_r^{(n)} = \{\hat{\delta}_{t,r}^{(n)}\}_{t=1}^T$ across all analyses, where the first subscript in $\hat{\delta}_{t,r}^{(n)}$ indexes the analysis and the second denotes the Monte Carlo iteration. We index all components of the MLE $\hat{\boldsymbol{\delta}}_r^{(n)}$ by the sample size $n = n_1$ for the first analysis, but note that the MLE $\hat{\delta}_{t,r}^{(n)}$ is in fact based on $n_t = c_t n$ observations. The constants $\{c_t\}_{t=1}^T$ are omitted from our notation for the joint MLE for simplicity. As with the sampling distribution of $\tau_*(\mathcal{D}_n)$ described in Section 2, we emphasize that we consider the sampling distribution of the MLE, $\hat{\boldsymbol{\delta}}_r^{(n)}$, irrespective of the interim decisions. Under the MLE regularity conditions in [van der Vaart \(1998\)](#), the approximate joint sampling distribution of the *complete* set of observable MLEs, $\hat{\boldsymbol{\delta}}_r^{(n)} \mid \boldsymbol{\theta} = \boldsymbol{\theta}_r$, is

$$\hat{\boldsymbol{\delta}}_r^{(n)} \sim \mathcal{N}\left(\boldsymbol{\delta}_r \times \mathbf{1}_T, \frac{\sigma_r^2}{n} \times \mathbf{C}\right), \quad (8)$$

where $\delta_r = \delta(\boldsymbol{\theta}_r)$ and the (i, j) -entry of the matrix \mathbf{C} is $c_{i,j} = \min\{c_i^{-1}, c_j^{-1}\}$ for $i, j \in \{1, \dots, T\}$. The result in (8) is based on the joint canonical distribution (Jennison and Turnbull, 1999) in sequential design theory. To develop our proxies used for theoretical purposes, we use conditional cumulative distribution function (CDF) inversion to map realizations from this T -dimensional multivariate normal distribution to points $\mathbf{u} = \{u_t\}_{t=1}^T \in [0, 1]^T$. For iteration r , we obtain the first component $\hat{\delta}_{1,r}^{(n)}$ of the maximum likelihood estimate as the u_1 -quantile of the sampling distribution of $\hat{\delta}_1^{(n)} \mid \boldsymbol{\theta}_r$. For the remaining components, we obtain $\hat{\delta}_{t,r}^{(n)}$ as the u_t -quantile of the sampling distribution of $\hat{\delta}_t^{(n)} \mid \{\hat{\delta}_s^{(n)} = \hat{\delta}_{s,r}^{(n)}\}_{s=1}^{t-1}, \boldsymbol{\theta}_r$.

Implementing this process with R points $\{\mathbf{u}_r\}_{r=1}^R \sim \mathcal{U}([0, 1]^T)$ and parameter values $\{\boldsymbol{\theta}_r\}_{r=1}^R \sim \Psi$ gives rise to a sample from the approximate sampling distribution of $\hat{\boldsymbol{\delta}}^{(n)}$ according to Ψ . For theoretical purposes, we substitute this sample $\{\hat{\boldsymbol{\delta}}_r^{(n)}\}_{r=1}^R$ into the posterior approximation in (7) to yield a proxy sample of posterior probabilities. For each analysis t , we approximate the probability in the t^{th} row of $\boldsymbol{\tau}(\mathcal{D}_n)$ as

$$\tau_{t,r}^{(n)} = \Phi\left(\frac{\delta_U - \hat{\delta}_{t,r}^{(n)}}{\sqrt{\sigma_r^2/c_t n}}\right) - \Phi\left(\frac{\delta_L - \hat{\delta}_{t,r}^{(n)}}{\sqrt{\sigma_r^2/c_t n}}\right) \quad (9)$$

where $\Phi(\cdot)$ is the standard normal CDF. The collection of $\{\tau_{t,r}^{(n)}\}_{t=1}^T$ values corresponding to $\{\mathbf{u}_r\}_{r=1}^R \sim \mathcal{U}([0, 1]^T)$ and $\{\boldsymbol{\theta}_r\}_{r=1}^R \sim \Psi$ define our proxy to the joint sampling distribution of $\boldsymbol{\tau}(\mathcal{D}_n)$. Under the predictive approach, there are two sources of randomness in the proxy sampling distribution of $\boldsymbol{\tau}(\mathcal{D}_n)$. The first source is associated with the parameter values $\boldsymbol{\theta}_r$ for iteration r . The second source is related to the point \mathbf{u}_r used to generate the maximum likelihood estimate $\hat{\boldsymbol{\delta}}_r^{(n)} \mid \boldsymbol{\theta}_r$, which serves as a conduit for the data $\mathcal{D}_{n,r}$.

When conditioning on particular values of \mathbf{u}_r and $\boldsymbol{\theta}_r$, the value of $\tau_{t,r}^{(n)} \mid \tau_{t-1,r}^{(n)}$ is no longer a stochastic quantity. For $t = 1$, the conditioning set $\tau_{t-1,r}^{(n)}$ is empty. We consider $\tau_{t,r}^{(n)}$ conditional on $\tau_{t-1,r}^{(n)}$ to model dependence in the joint proxy sampling distribution, and posterior summaries from previous stages do not provide additional information once $\tau_{t-1,r}^{(n)}$ is known. Given values of \mathbf{u}_r and $\boldsymbol{\theta}_r$, $\tau_{t,r}^{(n)} \mid \tau_{t-1,r}^{(n)}$ based on (9) is therefore a deterministic function of n . Lemma 1 provides a standard structure for these deterministic functions under general conditions.

Lemma 1. *For any $\boldsymbol{\theta}_r \sim \Psi$, let the model $p(y \mid \boldsymbol{\theta}_r)$ satisfy the conditions for the asymptotic normality of the complete distribution of the MLE and the prior $p(\boldsymbol{\theta})$ satisfy those for the BvM theorem. We consider a given point $\mathbf{u}_r \in [0, 1]^T$, $\boldsymbol{\theta}_r$ value, and distribution for any potential covariates \mathbf{X} . We suppose the sample sizes for the analyses are such that $\{n_t\}_{t=1}^T = n \times \{1, c_2, \dots, c_T\}$ for constants $\{c_t\}_{t=2}^T > 1$. For $t = 1, \dots, T$, the functions in (9) are such that*

$$\tau_{t,r}^{(n)} \mid \tau_{t-1,r}^{(n)} = \Phi(f_t(\delta_U, \boldsymbol{\theta}_r)\sqrt{n} + g_t(\mathbf{u}_r)) - \Phi(f_t(\delta_L, \boldsymbol{\theta}_r)\sqrt{n} + g_t(\mathbf{u}_r)), \quad (10)$$

where $f_t(\cdot)$ and $g_t(\cdot)$ are functions that do not depend on n .

We prove Lemma 1 and derive expressions for $\tau_{t,r}^{(n)} \mid \tau_{t-1,r}^{(n)}$ in Appendix A.1 of the online supplement. We use the result from (10) in the next subsection to prove new theoretical results about our proxy sampling

distributions that allow us to greatly expedite the design of Bayesian sequential experiments. In Section 3.2, we also extend the theory introduced here to create a proxy for the joint sampling distribution of posterior predictive probabilities in $\tau_P(\mathcal{D}_n)$. That proxy augments our proxy from this subsection to yield a proxy to the joint sampling distribution of posterior *and* posterior predictive probabilities in $\tau_*(\mathcal{D}_n)$.

3.2 Proxies to Posterior Predictive Probabilities

We now construct a proxy to the sampling distribution of posterior predictive probabilities that is also predicated on points $\{\mathbf{u}_r\}_{r=1}^R \sim \mathcal{U}([0, 1]^T)$ and parameter values $\{\boldsymbol{\theta}_r\}_{r=1}^R \sim \Psi$. This proxy again only theoretically motivates our design methodology proposed in Section 4. To develop this proxy, we must consider large-sample analogs for the components of the posterior predictive probability in (3). We illustrate how to create this proxy using $\tau_{P,t}(\mathcal{D}_n)$ from (4), the posterior predictive probability at analysis $t < T$. We condition on the $n_t = c_t n$ already-observed observations at this analysis, and the final analysis would include $n_* = n_T - n_t = (c_T - c_t)n$ future observations. Our conduit for these n_* observations generated from the posterior predictive distribution $p_P(y | \mathcal{D}_{n_t})$ is the maximum likelihood estimate $\hat{\delta}_{*,r}^{(n)}$. The conduit $\hat{\delta}_{*,r}^{(n)}$ is asymptotically sufficient in that – along with $\hat{\delta}_{t,r}^{(n)}$, n_t , and n_* – it determines the limiting posterior distribution of δ at the final analysis based on the current and future data. We derive this limiting posterior distribution below.

By the convolution of normal distributions, an approximate sampling distribution for the corresponding MLE $\hat{\delta}_{*,r}^{(n)}$ conditional on our conduit $\hat{\delta}_{t,r}^{(n)}$ for the data $\mathcal{D}_{n_t,r}$ is $\mathcal{N}(\hat{\delta}_{t,r}^{(n)}, \sigma_r^2/n_t + \sigma_r^2/n_*)$. The σ_r^2/n_t contribution to the variance comes from the large-sample approximation to the posterior distribution of δ in (7); this distribution is our analog to the current posterior $p(\boldsymbol{\theta} | \mathcal{D}_{n_t})$ that $p_P(y | \mathcal{D}_{n_t})$ integrates over. The σ_r^2/n_* contribution to the variance is related to the variability associated with a sample of n_* random observations from the model $p(y | \boldsymbol{\theta})$. The derived approximate sampling distribution for $\hat{\delta}_{*,r}^{(n)} | \hat{\delta}_{t,r}^{(n)}$ relies on the simplifying assumption that the variance σ_r^2 is the same for both data conduits $\hat{\delta}_{t,r}^{(n)}$ and $\hat{\delta}_{*,r}^{(n)}$. This assumption is sensible because our theoretical proxies are based on large-sample results, and σ_r^2 should be approximately constant once the sample size is large enough to precisely identify the true parameter values $\boldsymbol{\theta}_r$. This assumption fails in settings with time-varying parameters, which often invalidate the regularity conditions for the asymptotic normality of the MLE (van der Vaart, 1998).

The posterior distribution at the final analysis is based on a pooled sample of the initial data $\mathcal{D}_{n_t,r}$ and the n_* future observations. Our large-sample analog for this pooling process creates a pooled MLE by combining $\hat{\delta}_{t,r}^{(n)}$ and $\hat{\delta}_{*,r}^{(n)}$ using a weighted average. Based on the BvM theorem, the limiting posterior of δ at the final analysis is

$$\delta | \hat{\delta}_{t,r}^{(n)}, \hat{\delta}_{*,r}^{(n)} \sim \mathcal{N} \left(\frac{c_t}{c_T} \hat{\delta}_{t,r}^{(n)} + \frac{c_T - c_t}{c_T} \hat{\delta}_{*,r}^{(n)}, \frac{1}{n} \times \frac{\sigma_r^2}{c_T} \right). \quad (11)$$

The posterior predictive probability in (3) conditions on the data available at analysis t – but not the

future observations. The mean of the limiting posterior in (11) is thus a random quantity defined via the approximate distribution of $\hat{\delta}_{*,r}^{(n)} \mid \hat{\delta}_{t,r}^{(n)}$. Our large-sample analog to $\Pr\{\Pr(H_1 \mid \mathcal{D}_{nT}) \geq \gamma_T \mid \mathcal{D}_{n_{t,r}}\}$ involves quantiles of the limiting posterior of δ in (11). For any $q \in [0, 1]$, the q -quantile of this posterior is also a random quantity:

$$\lambda_r(q) = \frac{c_t}{c_T} \hat{\delta}_{t,r}^{(n)} + \frac{c_T - c_t}{c_T} \times \left(\hat{\delta}_{t,r}^{(n)} + Z \frac{\sigma_r}{\sqrt{n}} \sqrt{\frac{c_T}{c_t(c_T - c_t)}} \right) + \frac{1}{\sqrt{n}} \Phi^{-1}(q) \frac{\sigma_r}{\sqrt{c_T}}, \quad (12)$$

where $\hat{\delta}_{*,r}^{(n)}$ has been expressed as a function of a standard normal random variable Z .

Our analog to the posterior predictive probability in (3) is the probability that $\lambda_r(q_L) > \delta_L$ and $\lambda_r(q_L + \gamma_T) < \delta_U$ for some $q_L \in [0, 1 - \gamma_T]$. For one-sided hypotheses, this value for q_L does not depend on the sample size n : q_L is respectively 0 and $1 - \gamma_T$ when δ_U is ∞ and δ_L is $-\infty$. In Appendix A.2 of the online supplement, we show that the optimal value for $q_L \in [0, 1 - \gamma_T]$ approaches a constant as $n \rightarrow \infty$ in the case where both δ_L and δ_U are finite. Since we only use our large-sample proxies for theoretical purposes, we regard q_L as a constant that is independent of n .

By rearranging (12) to isolate for Z , we obtain the probability that $\lambda_r(q_L) > \delta_L$ and $\lambda_r(q_L + \gamma_T) < \delta_U$. This probability is our large-sample proxy to the probability in the t^{th} row of $\boldsymbol{\tau}_P(\mathcal{D}_n)$ for iteration r :

$$\tau_{P,t,r}^{(n)} = \Phi \left[\frac{\sqrt{n}(\delta_U - \hat{\delta}_{t,r}^{(n)})}{\sigma_r \sqrt{\frac{c_T - c_t}{c_t c_T}}} - \frac{\Phi^{-1}(q_L + \gamma_T)}{\sqrt{\frac{c_T - c_t}{c_t}}} \right] - \Phi \left[\frac{\sqrt{n}(\delta_L - \hat{\delta}_{t,r}^{(n)})}{\sigma_r \sqrt{\frac{c_T - c_t}{c_t c_T}}} - \frac{\Phi^{-1}(q_L)}{\sqrt{\frac{c_T - c_t}{c_t}}} \right]. \quad (13)$$

We now reintroduce the variability associated with the available data $\mathcal{D}_{n_{t,r}}$ to construct a proxy to the joint sampling distribution of $\boldsymbol{\tau}_P(\mathcal{D}_n)$. In Section 3.1, we described how conduits $\{\hat{\delta}_r^{(n)}\}_{r=1}^R$ for the data could theoretically be mapped to points $\{\mathbf{u}_r\}_{r=1}^R \sim \mathcal{U}([0, 1]^T)$ and parameter values $\{\boldsymbol{\theta}_r\}_{r=1}^R \sim \Psi$. The collection of $\{\tau_{P,t,r}^{(n)}\}_{t=1}^T$ values corresponding to these points and parameter values comprises our proxy to the sampling distribution of $\boldsymbol{\tau}_P(\mathcal{D}_n)$. Because our proxy to the sampling distribution of $\boldsymbol{\tau}(\mathcal{D}_n)$ is defined using the *same* points $\{\mathbf{u}_r\}_{r=1}^R$ and parameter values $\{\boldsymbol{\theta}_r\}_{r=1}^R$, we have constructed a proxy to the joint sampling distribution of posterior and posterior predictive probabilities in $\boldsymbol{\tau}_*(\mathcal{D}_n)$. When conditioning on values of \mathbf{u}_r and $\boldsymbol{\theta}_r$, $\tau_{P,t,r}^{(n)} \mid \tau_{t,r}^{(n)}$ based on (13) is a deterministic function of n . Lemma 2 provides a standard form for these functions. We prove this lemma and derive expressions for $\tau_{P,t,r}^{(n)} \mid \tau_{t,r}^{(n)}$ that account for dependence in the joint proxy sampling distribution in Appendix A.2 of the supplement.

Lemma 2. *We suppose the conditions for Lemma 1 are satisfied. We consider a given point $\mathbf{u}_r \in [0, 1]^T$, $\boldsymbol{\theta}_r$ value, and distribution for any potential covariates \mathbf{X} . For $t = 1, \dots, T - 1$, the functions in (13) are such that*

$$\tau_{P,t,r}^{(n)} \mid \tau_{t,r}^{(n)} = \Phi(f_{P,t}(\delta_U, \boldsymbol{\theta}_r)\sqrt{n} + g_{P,t}(\mathbf{u}_r, q_L + \gamma_T)) - \Phi(f_{P,t}(\delta_L, \boldsymbol{\theta}_r)\sqrt{n} + g_{P,t}(\mathbf{u}_r, q_L)), \quad (14)$$

where $f_{P,t}(\cdot)$ and $g_{P,t}(\cdot)$ are functions that do not depend on n .

Our proxy to the sampling distribution of $\tau_*(\mathcal{D}_n)$ relies on asymptotic results, so it may differ materially from the true sampling distribution for finite n . Therefore, this proxy only motivates our theoretical result in Theorem 1, which utilizes the deterministic functions derived in Lemmas 1 and 2. Theorem 1 guarantees that the logits of $\tau_{t,r}^{(n)} \mid \tau_{t-1,r}^{(n)}$ and $\tau_{P,t,r}^{(n)} \mid \tau_{t,r}^{(n)}$ are approximately linear functions of n for all $t \in \{1, \dots, T\}$. We later adapt this result to estimate the error rates of a sequential design across a wide range of sample sizes by estimating the true sampling distribution of $\tau_*(\mathcal{D}_n)$ at only two values of n .

Theorem 1. *We suppose the conditions for Lemma 1 are satisfied. Define $\text{logit}(x) = \log(x) - \log(1-x)$. We consider a given point $\mathbf{u}_r \in [0, 1]^T$, $\boldsymbol{\theta}_r$ value, and distribution for any potential covariates \mathbf{X} . The functions $\{\tau_{t,r}^{(n)} \mid \tau_{t-1,r}^{(n)}\}_{t=1}^T$ based on (10) and $\{\tau_{P,t,r}^{(n)} \mid \tau_{t,r}^{(n)}\}_{t=1}^{T-1}$ based on (14) are such that*

$$(a) \lim_{n \rightarrow \infty} \frac{d}{dn} \text{logit}(\tau_{t,r}^{(n)} \mid \tau_{t-1,r}^{(n)}) = (0.5 - \mathbb{I}\{\delta_r \notin (\delta_L, \delta_U)\}) \times \min\{f_t(\delta_U, \boldsymbol{\theta}_r)^2, f_t(\delta_L, \boldsymbol{\theta}_r)^2\}.$$

$$(b) \lim_{n \rightarrow \infty} \frac{d}{dn} \text{logit}(\tau_{P,t,r}^{(n)} \mid \tau_{t,r}^{(n)}) = (0.5 - \mathbb{I}\{\delta_r \notin (\delta_L, \delta_U)\}) \times \min\{f_{P,t}(\delta_U, \boldsymbol{\theta}_r)^2, f_{P,t}(\delta_L, \boldsymbol{\theta}_r)^2\}.$$

Theorem 1 is novel to this paper; we prove parts (a) and (b) in Appendix B of the supplement. We now discuss the practical implications of this theorem. The limiting derivatives in parts (a) and (b) are constants that do not depend on n . Moreover, these limiting derivatives do not depend on the point \mathbf{u}_r which controls the dependence within the joint proxy sampling distribution of $\tau_*(\mathcal{D}_n)$. The limiting derivatives of (i) $\text{logit}(\tau_{t,r}^{(n)})$ and $\text{logit}(\tau_{t,r}^{(n)} \mid \tau_{t-1,r}^{(n)})$ and (ii) $\text{logit}(\tau_{P,t,r}^{(n)})$ and $\text{logit}(\tau_{P,t,r}^{(n)} \mid \tau_{t,r}^{(n)})$ are therefore the same. In the joint proxy sampling distribution, the linear approximations to $l_{t,r}^{(n)} = \text{logit}(\tau_{t,r}^{(n)} \mid \tau_{t-1,r}^{(n)})$ and $l_{P,t,r}^{(n)} = \text{logit}(\tau_{P,t,r}^{(n)} \mid \tau_{t,r}^{(n)})$ as functions of n are thus good global approximations for large sample sizes. These linear approximations should be locally suitable for a range of smaller sample sizes.

Under the conditional approach where $\{\boldsymbol{\theta}_r\}_{r=1}^R$ are the same, the (conditional) quantiles of the sampling distributions of $l_{t,r}^{(n)}$ and $l_{P,t,r}^{(n)}$ therefore change linearly as a function of n . In Section 4, we adapt this linear trend in the proxy sampling distribution to flexibly model the logits of $\tau_*(\mathcal{D}_n)$ as linear functions of n when independently simulating samples $\mathcal{D}_{n,r}$ according to $\boldsymbol{\theta}_r \sim \Psi$ under the conditional or predictive approach. Although the proxy sampling distribution is predicated on asymptotic results for the first analysis, we illustrate the good performance of our design procedure with finite sample sizes n in Section 5.

4 Efficient Design of Group Sequential Experiments

We generalize the results from Theorem 1 to develop a procedure to choose sample sizes and tune decision thresholds for Bayesian group sequential designs in Algorithm 1. This procedure requires that we estimate the complete sampling distribution of posterior summaries $\tau_*(\mathcal{D}_n)$ by simulating data \mathcal{D}_n at *only* two values of n : n_a and n_b . The initial sample size for the first analysis n_a can be selected based on the anticipated budget for the sequential experiment. In Algorithm 1, we add a subscript to $\mathcal{D}_{n,r}$ between n and r that distinguishes whether the data are generated according to the model Ψ_0 or Ψ_1 defined in Section 2. In

addition to the choices discussed previously, we specify a distribution with parameters ζ for any potential covariates $\mathbf{X}_{n_t \times w}$. The example in Section 5.1 elaborates on design with additional covariates. We also define criteria for the error rates. Under Ψ_1 where H_1 is true, we want $\mathbb{E}_{\Psi_1}[\Pr(\nu(\mathcal{D}_n) = 1 \mid \boldsymbol{\theta})] \geq \Gamma_1$. We want $\mathbb{E}_{\Psi_0}[\Pr(\nu(\mathcal{D}_n) = 1 \mid \boldsymbol{\theta})] \leq \Gamma_0$ under Ψ_0 where H_0 is true. Algorithm 1 details a general application of our methodology with the conditional approach, and we later describe potential modifications.

Algorithm 1 Procedure to Determine Sample Sizes and Decision Thresholds

```

1: procedure DESIGN( $p(y \mid \boldsymbol{\theta})$ ,  $\delta(\cdot)$ ,  $\delta_L$ ,  $\delta_U$ ,  $p(\boldsymbol{\theta})$ ,  $\Psi_0$ ,  $\Psi_1$ ,  $R$ ,  $M$ ,  $n_a$ ,  $\{c_t\}_{t=1}^T$ ,  $\zeta$ ,  $\Gamma_0$ ,  $\Gamma_1$ )
2:   Compute  $\{\boldsymbol{\tau}_*(\mathcal{D}_{n_a,0,r})\}_{r=1}^R$  obtained with  $\boldsymbol{\theta}_r \sim \Psi_0$ .
3:   Choose thresholds from  $\boldsymbol{\gamma}$ ,  $\boldsymbol{\xi}$ ,  $\boldsymbol{\eta}$ , and  $\boldsymbol{\rho}$  to ensure  $R^{-1} \sum_{r=1}^R \mathbb{I}\{\nu(\mathcal{D}_{n_a,0,r}) = 1\} \leq \Gamma_0$ .
4:   Compute  $\{\boldsymbol{\tau}_*(\mathcal{D}_{n_a,1,r})\}_{r=1}^R$  obtained with  $\boldsymbol{\theta}_r \sim \Psi_1$ .
5:   If  $R^{-1} \sum_{r=1}^R \mathbb{I}\{\nu(\mathcal{D}_{n_a,1,r}) = 1\} \geq \Gamma_1$ , choose  $n_b < n_a$ . If not, choose  $n_b > n_a$ .
6:   Compute  $\{\boldsymbol{\tau}_*(\mathcal{D}_{n_b,1,r})\}_{r=1}^R$  obtained with  $\boldsymbol{\theta}_r \sim \Psi_1$ .
7:   for  $d$  in  $1:R$  do
8:     for  $t$  in  $1:T$  do
9:       Let the sample  $\mathcal{D}_{n_a,1,r}$  correspond to the  $d^{\text{th}}$  order statistic of  $\{l_t(\mathcal{D}_{n_a,1,r})\}_{r=1}^R$ .
10:      Pair the  $d^{\text{th}}$  order statistics of  $\{l_t(\mathcal{D}_{n_a,1,r})\}_{r=1}^R$  and  $\{l_t(\mathcal{D}_{n_b,1,r})\}_{r=1}^R$  with linear approximations
        to obtain  $\hat{l}_t(\mathcal{D}_{n,1,r})$  estimates for new  $n$  values.
11:      if  $t < T$  then
12:        Repeat Lines 9 and 10 with  $\{l_{P,t}(\mathcal{D}_{n_a,1,r})\}_{r=1}^R$  and  $\{l_{P,t}(\mathcal{D}_{n_b,1,r})\}_{r=1}^R$  to estimate  $\hat{l}_{P,t}(\mathcal{D}_{n,1,r})$ 
          for new  $n$ .
13:      Obtain  $\{\hat{\boldsymbol{\tau}}_*(\mathcal{D}_{n,1,r})\}_{r=1}^R$  as the inverse logits of the estimates  $\{\hat{l}_t(\mathcal{D}_{n,1,r})\}_{t=1}^T$  and  $\{\hat{l}_{P,t}(\mathcal{D}_{n,1,r})\}_{t=1}^{T-1}$ .
14:      Find  $n_c$ , the smallest  $n \in \mathbb{Z}^+$  such that  $R^{-1} \sum_{r=1}^R \mathbb{I}\{\hat{\nu}(\mathcal{D}_{n,1,r}) = 1\} \geq \Gamma_1$ .
15:      return  $n_c$  as recommended  $n$ 

```

We now elaborate on several steps of Algorithm 1. In Line 3, we choose suitable vectors for the relevant decision thresholds to ensure the estimate for $\mathbb{E}_{\Psi_0}[\Pr(\nu(\mathcal{D}_n) = 1 \mid \boldsymbol{\theta})]$ based on (6) is at most Γ_0 . Initial values for the success thresholds $\boldsymbol{\gamma}$ and $\boldsymbol{\eta}$ can be chosen using standard theory from group sequential designs (Jennison and Turnbull, 1999), and the failure thresholds $\boldsymbol{\xi}$ and $\boldsymbol{\rho}$ can generally be initialized as low probabilities. While implementing Algorithm 1, the choices for $\boldsymbol{\gamma}$, $\boldsymbol{\xi}$, $\boldsymbol{\eta}$, and $\boldsymbol{\rho}$ may be tuned using sampling distribution estimates obtained under Ψ_0 and Ψ_1 . Because Algorithm 1 efficiently estimates sampling distributions across a broad range of sample sizes, our methodology helps streamline this tuning process. We provide several illustrations of how to tune the decision thresholds in Section 5.

All posterior summaries approximated in Lines 2 to 6 of Algorithm 1 are obtained by simulating data given parameter values from Ψ_0 or Ψ_1 . Lines 7 and 8 compute logits of these summaries under Ψ_1 : $l_t(\mathcal{D}_{n,1,r}) = \text{logit}(\boldsymbol{\tau}_t(\mathcal{D}_{n,1,r}))$ and $l_{P,t}(\mathcal{D}_{n,1,r}) = \text{logit}(\boldsymbol{\tau}_{P,t}(\mathcal{D}_{n,1,r}))$. If not all components of the joint sampling distribution of posterior summaries inform decision rules in a particular design, various rows in $\boldsymbol{\tau}_*(\mathcal{D}_n)$ may be ignored.

We recommend calculating posterior summaries using nonparametric kernel density estimates so that these logits are finite. These posterior summaries and their logits account for the analysis prior $p(\boldsymbol{\theta})$ because our method is based on simulation; however, Algorithm 1 must be reimplemented to consider different choices for $p(\boldsymbol{\theta})$.

We construct linear approximations separately for each summary using logits corresponding to sample sizes n_a and n_b under the model Ψ_1 in Lines 7 to 12. This second sample size n_b could be chosen as the smallest sample size n such that power is sufficiently large when the sampling distribution of $\boldsymbol{\tau}_*(\mathcal{D}_n)$ is modeled using lines that pass through $(n_a, \hat{l}_t(\mathcal{D}_{n_a,1,r}))$ or $(n_a, \hat{l}_{P,t}(\mathcal{D}_{n_a,1,r}))$ with the limiting slopes from Theorem 1 (see [Hagar and Stevens \(2025\)](#) for more details). Alternatively, n_b could be chosen to explore a range of relevant sample sizes between n_a and n_b . We elaborate on the choice of n_a and n_b for our examples in Section 5. We use these linear approximations to estimate logits of posterior summaries for new values of n as $\hat{l}_t(\mathcal{D}_{n,1,r})$ or $\hat{l}_{P,t}(\mathcal{D}_{n,1,r})$. We place a hat over the l here to convey that this logit was estimated using a linear approximation instead of a sample of data. To maintain the proper level of dependence in the joint sampling distribution of $\boldsymbol{\tau}_*(\mathcal{D}_n)$, we group the linear functions from Lines 10 and 12 across all posterior summaries based on the sample $\mathcal{D}_{n_a,1,r}$ that defined the linear approximations.

Given the linear trend in the proxy sampling distribution quantiles discussed in Section 3.2, these linear approximations can be constructed based on order statistics of estimates of the true sampling distributions under the conditional approach. Because Theorem 1 ensures that the limiting slopes of (i) $\text{logit}(\tau_{t,r}^{(n)})$ and $\text{logit}(\tau_{t,r}^{(n)} \mid \tau_{t-1,r}^{(n)})$ and (ii) $\text{logit}(\tau_{P,t,r}^{(n)})$ and $\text{logit}(\tau_{P,t,r}^{(n)} \mid \tau_{t,r}^{(n)})$ from the proxy sampling distribution are the same, we use the *marginal* sampling distributions for each row of $\boldsymbol{\tau}_*(\mathcal{D}_n)$ to estimate slopes for the *conditional* logits. Under the predictive approach, the process in Lines 7 to 12 can be modified. We split the logits of the posterior summaries for each n value into subgroups based on the order statistics of their δ_r values before constructing the linear approximations. In Line 14, we find the smallest value of n such that our estimate for $\mathbb{E}_{\Psi_1}[\Pr(\nu(\mathcal{D}_n) = 1 \mid \boldsymbol{\theta})]$ based on the indicators $\{\hat{\nu}(\mathcal{D}_{n,1,r})\}_{r=1}^R$ that correspond to $\{\hat{\boldsymbol{\tau}}_*(\mathcal{D}_{n,1,r})\}_{r=1}^R$ is at least Γ_1 . Sample sizes throughout the sequential design are obtained using the constants $\{c_t\}_{t=2}^T$.

We did not estimate the sampling distribution of $\boldsymbol{\tau}_*(\mathcal{D}_{n_b})$ under Ψ_0 in Algorithm 1. To consider the worst-case error rates, it is common practice to consider Ψ_0 models that assign all weight to $\boldsymbol{\theta}_r$ values such that $\delta(\boldsymbol{\theta}_r)$ equals δ_L or δ_U . We show that all limiting slopes in part (b) of Theorem 1 are zero for such models Ψ_0 in Appendix B of the online supplement; the type I error rate is thus approximately constant across a range of large n values. If using a more general model Ψ_0 , Algorithm 1 can be adapted to implement the process in Lines 6 to 13 under Ψ_0 to efficiently estimate the sampling distribution of $\boldsymbol{\tau}_*(\mathcal{D}_n)$ for new values of n . These estimated sampling distributions could be used to further tune the decision thresholds $\boldsymbol{\gamma}$, $\boldsymbol{\xi}$, $\boldsymbol{\eta}$, and $\boldsymbol{\rho}$. We evaluate the performance of Algorithm 1 for two example designs in Section 5.

5 Performance for Example Designs

5.1 PLATINUM-CAN Trial

We first assess the performance of our method with example designs based on the Canadian placebo-controlled randomized trial of tecovirimat in non-hospitalized patients with Mpox (PLATINUM-CAN) (Klein, 2024). This trial employs a fixed design with a single frequentist analysis at the end of the trial. For illustration, we consider various Bayesian group sequential designs with between one and four interim analyses. The main goal of the trial is to establish that the antiviral drug tecovirimat reduces the duration of illness associated with Mpox infection. The trial’s primary outcome used for sample size determination is the time to lesion resolution, defined as the first day after randomization on which all Mpox lesions are resolved. The impact of tecovirimat on the time to lesion resolution will be evaluated in comparison to a placebo, with balanced randomization to the two arms.

We model the time to lesion resolution using a Bayesian proportional hazards model, where the baseline “hazard” of experiencing lesion resolution is a piecewise constant function. The model adjusts for a binary covariate that indicates whether patients were randomized to an arm within 7 days of Mpox symptom onset. The target of inference $\delta(\boldsymbol{\theta})$ for this trial is the population-level rate ratio of experiencing lesion resolution. The rate ratio is akin to the hazard ratio but for desirable outcomes, such as lesion resolution. Full details on the analysis model and its parameters $\boldsymbol{\theta}$, the selected prior distributions, and the marginalization procedure to obtain the population-level rate ratio are given in Appendix D.1 of the supplement.

The hypotheses for this trial are $H_0 : \delta \leq 1$ vs. $H_1 : \delta > 1$. That is, $\delta_L = 1$ and $\delta_U = \infty$. We consider two sets of spacings $\mathbf{c} = (c_1, c_2, c_3, c_4, c_5)$ for the interim analyses: one where the analyses are backloaded such that $\mathbf{c} = (1, 1.5, 2, 2.5, 3)$ and another where the analyses are equally spaced such that $\mathbf{c} = (1, 2, 3, 4, 5)$. For designs with $T < 5$ planned analyses, only the constants $\{c_t\}_{t=1}^T$ are considered. This example only accommodates early stopping for success based on posterior probabilities. Across all analyses, we want the type I error rate to be at most $\Gamma_0 = 0.025$ and power to be at least $\Gamma_1 = 0.8$. For this example, we do not have decision thresholds $\boldsymbol{\xi}$, $\boldsymbol{\eta}$, or $\boldsymbol{\rho}$. We tune the success thresholds $\boldsymbol{\gamma}$ by setting the initial values of $\{\gamma_t\}_{t=1}^{T-1}$ to those obtained from an alpha-spending function (Demets and Lan, 1994) that approximates the O’Brien-Fleming boundaries (O’Brien and Fleming, 1979). The final threshold γ_T is chosen as the smallest probability that maintains a type I error rate of 0.025 based on the sampling distribution estimate of $\boldsymbol{\tau}(\mathcal{D}_n)$ under Ψ_0 in Line 2 of Algorithm 1. Alternative methods could also be used to tune the decision thresholds, ranging from simpler methods that enforce $\gamma_1 = \dots = \gamma_T$ to more complex ones.

Our process to simulate lesion resolution times and patient dropout is described thoroughly in Appendix D.1 of the supplement. Here we overview the models Ψ_0 and Ψ_1 that govern the data generation process for H_0 and H_1 under the conditional approach. For both Ψ_0 and Ψ_1 , approximately 23% of patients in the control arm have active lesions at the end of the 28-day observation period; the resolution times for

those patients are right censored at 28 days. Under Ψ_1 , the lesion resolution times are simulated to attain a population-level rate ratio of 1.3. Roughly 10% of patients drop out before experiencing lesion resolution and before day 28. The resolution times for those patients are right censored at their last-attended visit. For illustration, the baseline hazards and censoring process detailed in Appendix D.1 are held constant for all settings we consider.

In all settings, Algorithm 1 was implemented with $R = 10^4$ iterations and sample sizes of $n_a = 200$ and $n_b = 400$. Since the earlier c_t values are the same for all T considered within a given set of analysis spacings, we implement Algorithm 1 once with $T = 5$ for each set of spacings. For designs with $T < 5$, we ignore the later stages of the sampling distribution modeled using linear approximations in Algorithm 1. We chose the sample sizes n_a and n_b based on PLATINUM-CAN to explore designs with varying power across the T values considered. Figure 1 visualizes the cumulative stopping probability at each analysis with respect to n for all settings given our choice for Ψ_1 . The solid blue and green curves were *estimated* using linear approximations to logits of posterior probabilities at only two sample sizes (n_a and n_b) using the process in Lines 4 to 12 of Algorithm 1. The short-dashed curves represent pointwise 95% bootstrap confidence intervals for the cumulative stopping probabilities. We describe how to construct these bootstrap confidence intervals in Appendix C. The red and black long-dashed curves were *simulated* by independently generating samples \mathcal{D}_n to estimate sampling distributions of $\tau(\mathcal{D}_n)$ at $n = \{100, 150, \dots, 500\}$. In Figure 1, the stopping probabilities for the designs with equally spaced and backloaded analyses consider different ranges of sample sizes for n_t , $t \geq 2$ because $\{c_t\}_{t=2}^T$ differ for the two settings.

Although the long-dashed curves are impacted by simulation variability, we use them as surrogates for the true stopping probabilities. We observe good alignment between the solid curves estimated using linear approximations and the long-dashed ones obtained by independently simulating samples. Apart from slight deviations at the smaller sample sizes in Figure 1, the long-dashed curves are generally contained within the pointwise 95% bootstrap confidence intervals. The agreement between the solid and long-dashed curves could be improved for smaller sample sizes (i.e., for n that are far outside the range between n_a and n_b) if we also estimated the sampling distribution of posterior summaries at a third sample size $n_c < n_a$. We could use Algorithm 1 with the two sampling distribution estimates at n_c and n_a to explore sample sizes $n < n_a$, and our existing linear approximations could be used to consider $n \geq n_a$. However, we have found that it is generally not necessary to approximate the sampling distribution of posterior summaries at a third sample size, particularly when only considering one value of T per implementation of Algorithm 1.

The solid curves in Figure 1 are substantially easier to obtain since we need only estimate the sampling distribution of $\tau(\mathcal{D}_n)$ at two values of n . Even so, it took roughly 40 minutes on a high-computing server to estimate all solid curves for each set of analysis spacings in Figure 1 when approximating each posterior using Markov chain Monte Carlo with one chain where the first 1000 iterations were discarded as burnin

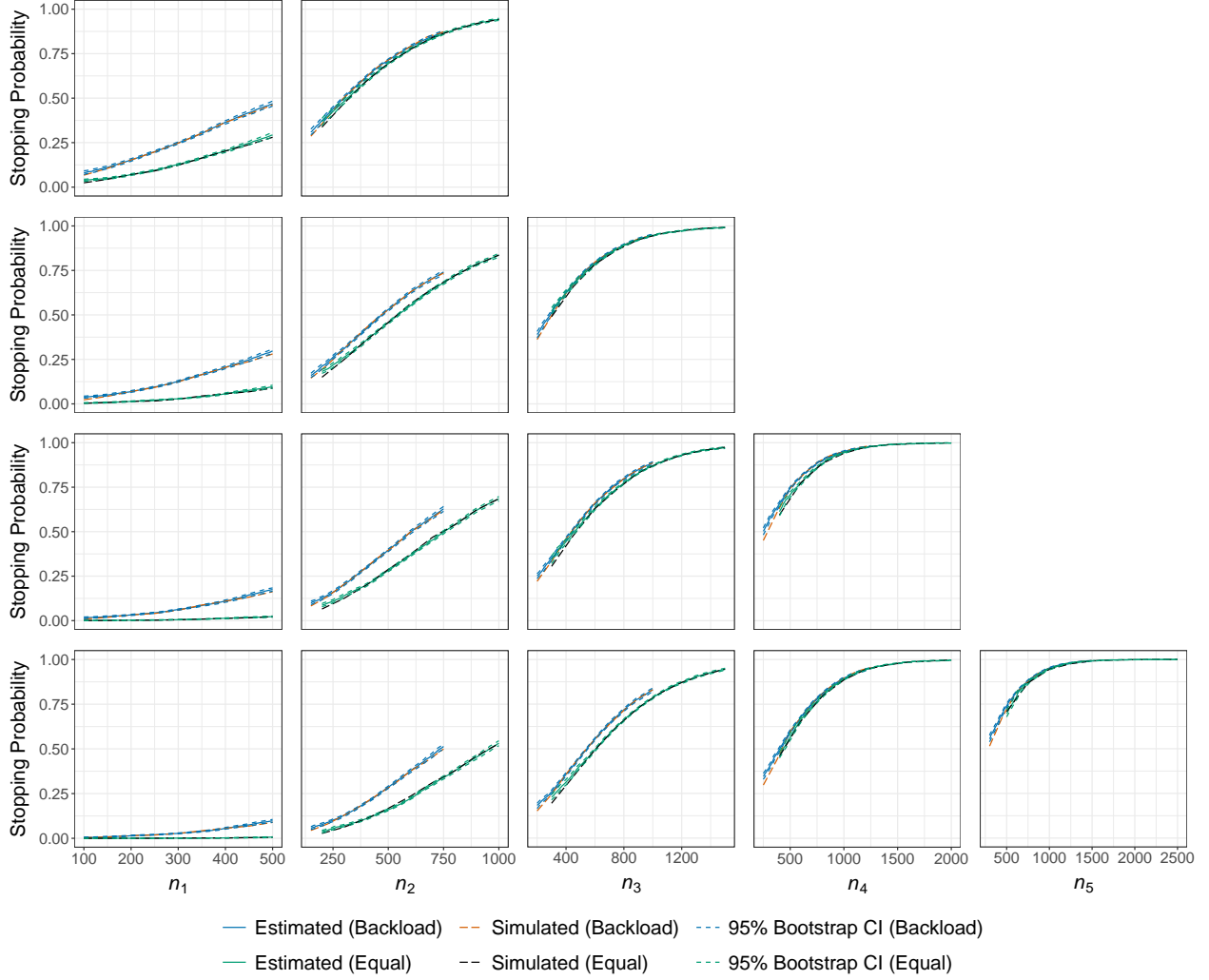


Figure 1: The cumulative stopping probabilities under Ψ_1 for the PLATINUM-CAN example. Column t represents analysis t and row T represents a design with T planned analyses.

and the next 10^4 iterations were retained. While initial simulations used multiple Markov chains to verify convergence for all numerical studies in this paper, our large-scale simulations employed less intensive settings that achieved reasonable convergence. We considered 9 values of n to simulate the long-dashed curves in Figure 1 for each set of analysis spacings, taking roughly 3 hours using the same computing resources. The computational savings of our method scale with the number of sample sizes at which the sampling distribution of posterior summaries is estimated. If a standard method estimates sampling distributions at Q values of n , then our approach is $Q/2$ times faster. Unlike standard methods, our approach allows practitioners to assess error rates for new values of n without conducting additional simulations.

Numerical results for both sets of analysis spacings under Ψ_0 and Ψ_1 are summarized in Table 1. These cumulative stopping probabilities were obtained using confirmatory simulations to estimate the joint sampling distribution of $\tau(\mathcal{D}_n)$ at $\{n_t\}_{t=1}^T = n \times \{c_t\}_{t=1}^T$, where the sample size $n = n_1$ was recommended using the

linear approximations from Algorithm 1. All non-integer sample sizes were rounded up to the nearest whole number. While simulation variability impacts the sampling distribution estimates used for confirmatory purposes and those used to tune the decision thresholds in Algorithm 1, power at the final analysis for each design is roughly $\Gamma_1 = 0.8$ and the overall type I error rate is approximately $\Gamma_0 = 0.025$, demonstrating the strong performance of our method. The recommended decision thresholds and expected total sample sizes for each design are reported in Appendix D.1 of the supplement. Additional simulations based on PLATINUM-CAN that further illustrate the utility of our approach are described in Appendix D.2.

Spacing	n	T	Model	Cumulative Stopping Probability				
				$t = 1$	$t = 2$	$t = 3$	$t = 4$	$t = 5$
Backload	412	2	Ψ_1	0.3891	0.8087			
			Ψ_0	0.0050	0.0288			
	306	3	Ψ_1	0.1333	0.4948	0.8111		
			Ψ_0	0.0009	0.0077	0.0281		
	234	4	Ψ_1	0.0379	0.2571	0.5417	0.8002	
			Ψ_0	0.0002	0.0022	0.0091	0.0289	
	197	5	Ψ_1	0.0186	0.1264	0.3543	0.5787	0.8000
			Ψ_0	0.0002	0.0015	0.0047	0.0119	0.0283
Equal	319	2	Ψ_1	0.1444	0.8035			
			Ψ_0	0.0008	0.0195			
	208	3	Ψ_1	0.0221	0.3875	0.8037		
			Ψ_0	0.0002	0.0057	0.0241		
	161	4	Ψ_1	0.0071	0.1524	0.5268	0.8160	
			Ψ_0	0.0001	0.0012	0.0080	0.0242	
	125	5	Ψ_1	0.0047	0.0479	0.2828	0.5736	0.8084
			Ψ_0	0.0000	0.0003	0.0025	0.0086	0.0226

Table 1: Stopping probabilities at the recommended n values for the PLATINUM-CAN example obtained by simulating confirmatory estimates of sampling distributions.

5.2 Quality Control for Decaffeinated Coffee

We next assess the performance of our method with an example design based on quality control for decaffeinated coffee. The U.S. Department of Agriculture requires that decaffeinated coffee beans retain at most 3% of their initial caffeine content after the decaffeination process. In this example, we suppose that a coffee producer wants to perform quality control on a revamped decaffeination process. High-performance liquid chromatography (HPLC) is the gold-standard method to measure the caffeine content in coffee beans (Ashoor et al., 1983). Since there can be substantial variability in the caffeine content across different batches of decaffeinated coffee output from the same manufacturing process (McCusker et al., 2006), samples of coffee beans from a variety of batches must be tested. A sequential quality control experiment that allows early stopping for both success and failure would mitigate the costs of HPLC (Ashoor et al., 1983) and the risk of producing unsellable coffee batches.

The datum collected from each coffee batch is the proportion of caffeine remaining. Because these proportions are close to zero in acceptable decaffeinated coffee beans, the MLE’s stability and the suitability

of the normal approximation to its sampling distribution may be questionable for small and moderate sample sizes. Bayesian analysis of the proportions is advantageous: it does not rely on asymptotic approximations to estimate posterior distributions and allows for the use of priors to improve stability when necessary. This example hence confirms the performance of our method with smaller sample sizes.

The proportions of residual caffeine obtained from the revamped decaffeination process are modeled using a beta distribution parameterized by shape parameters $\boldsymbol{\theta} = (\alpha, \beta)$. The target of inference $\delta(\boldsymbol{\theta})$ is the 0.99-quantile of this distribution: $\delta = F^{-1}(0.99; \alpha, \beta)$, where $F^{-1}(\cdot)$ is the inverse CDF of the beta distribution. The hypotheses for this experiment are $H_0 : \delta \geq 0.03$ vs. $H_1 : \delta < 0.03$. That is, we aim to conclude that the probability of producing an unsatisfactory batch of decaffeinated coffee beans is at most 0.01 using the interval endpoints $\delta_L = -\infty$ and $\delta_U = 0.03$.

We design this experiment with $T = 4$ analyses such that $c_2 = 1.5$, $c_3 = 2$, and $c_4 = 2.5$. We accommodate stopping for success based on posterior probabilities and stopping for failure based on posterior predictive probabilities. We want the cumulative type I error rate to be at most $\Gamma_0 = 0.1$ and power to be at least $\Gamma_1 = 0.8$. We do not have decision thresholds $\boldsymbol{\xi}$ or $\boldsymbol{\eta}$ for this example. For illustration, we fix the failure thresholds $\boldsymbol{\rho} = (0.1, 0.2, 0.3)$ and choose the success thresholds $\boldsymbol{\gamma} = (0.9990, 0.9952, 0.9903, 0.9322)$ by proportionally adjusting initial values for all components of $\boldsymbol{\gamma}$ toward 1 until the type I error rate based on the sampling distribution estimate of $\boldsymbol{\tau}_*(\mathcal{D}_n)$ in Line 2 of Algorithm 1 is at most 0.1.

To illustrate that the predictive and conditional approaches give rise to distinct sample size recommendations, we consider two Ψ_1 models. The predictive model Ψ_1 ensures that $\{\delta(\boldsymbol{\theta}_r)\}_{r=1}^R \sim \mathcal{U}(0.0225, 0.0275)$, and the conditional model Ψ_1 is such that $\delta(\boldsymbol{\theta}_r) = 0.025$ for all Monte Carlo iterations. Both Ψ_1 models are paired with a conditional Ψ_0 model that ensures $\delta(\boldsymbol{\theta}_r) = 0.03$ across all iterations. We elaborate on these choices for Ψ_1 and Ψ_0 and specify diffuse priors in Appendix E of the supplement. For both Ψ_1 models we consider, Algorithm 1 was implemented with $R = 10^4$ and $M = 10^3$ and sample sizes for the first analysis of $n_a = 38$ and $n_b = 18$. We chose these sample sizes to explore designs with maximum sample sizes ranging between 45 and 95. Under the predictive approach, the logits of posterior summaries were split into 10 subgroups based on the order statistics of their δ_r values before constructing the linear approximations.

It took roughly 15 hours on a high-computing server to implement Algorithm 1 for each Ψ_1 model when approximating each posterior using Markov chain Monte Carlo with one chain of 1000 burnin iterations and 5×10^3 retained iterations. Appendix E contains a plot similar to Figure 1 for this decaffeinated coffee example. We observed good alignment in that supplemental figure between our results based on linear approximations and those obtained by independently estimating the sampling distribution of $\boldsymbol{\tau}_*(\mathcal{D}_n)$ at various n values. It took roughly 2 days to explore the sample size space for each Ψ_1 model with independent sampling distribution estimates at six values of n between 18 and 38 using the same computing resources. Thus, estimating the sampling distribution of posterior summaries at only two values of n greatly expedites

the design process.

Numerical results for all data generation processes Ψ_0 and Ψ_1 are summarized in Table 2. These cumulative stopping probabilities were obtained using confirmatory simulations to estimate the sampling distribution of $\tau_*(\mathcal{D}_n)$ at $\{n_1, n_2, n_3, n_4\} = n \times \{1, 1.5, 2, 2.5\}$, where the sample size $n = n_1$ was recommended using the linear approximations from Algorithm 1. Our method recommends designs with suitable operating characteristics: power at the final analysis for the predictive and conditional approaches is approximately $\Gamma_1 = 0.8$, and the overall type I error rate is roughly $\Gamma_0 = 0.1$. Furthermore, we have a large cumulative probability of stopping for failure when H_0 is true but a small probability of stopping for failure under Ψ_1 . The expected sample size under Ψ_1 is 68.37 and 62.49 for predictive and conditional approaches, respectively.

Approach	n	Model	Cumulative Stopping Probability					
			Success				Failure	
			t = 1	t = 2	t = 3	t = 4	t = 1	t = 2
Predictive	36	Ψ_1	0.1081	0.3244	0.5171	0.8061	0.0379	0.0922
		Ψ_0	0.0060	0.0162	0.0305	0.1030	0.3652	0.6385
Conditional	32	Ψ_1	0.0849	0.2839	0.4834	0.8127	0.0340	0.0824
		Ψ_0	0.0058	0.0186	0.0350	0.1090	0.3592	0.6287

Table 2: Stopping probabilities at the recommended n values for the decaffeinated coffee example obtained by simulating confirmatory estimates of sampling distributions.

6 Discussion

In this paper, we proposed an economical framework to estimate error rates associated with decision procedures based on posterior and posterior predictive probabilities in group sequential designs. This framework determines the minimum sample sizes that ensure the power of the experiment is sufficiently large while tuning decision thresholds to bound the type I error rate. The computational efficiency of our framework is predicated on a proxy for the joint sampling distribution of posterior summaries across analyses irrespective of the interim decisions. We use the behaviour in this large-sample proxy to motivate estimating true sampling distributions at only two sample sizes. Our method significantly reduces the computational overhead required to design Bayesian group sequential experiments in a wide range of disciplines.

The methods proposed in this paper could be extended in various aspects to accommodate more complex sequential designs. Our work in this article constrained the sample sizes for the analyses to be such that $\{n_t\}_{t=1}^T = n \times \{1, c_2, \dots, c_T\}$ as the sample size n for the first analysis changes. This constraint precludes sequential designs that leverage response-adaptive randomization, including Thompson sampling (Thompson, 1933). Response-adaptive randomization is commonly incorporated into clinical trials and multi-armed bandit experiments (Katehakis and Veinott Jr, 1987) more generally. Future research could consider how to efficiently implement these extensions.

Moreover, the proxy sampling distributions introduced in this article rely on large-sample regularity

conditions. The regularity conditions for the asymptotic normality of the MLE prevent us from considering designs with time-varying parameters. The conditions for the BvM theorem might also be violated if using certain methods to dynamically incorporate prior information into Bayesian sequential designs. The ability to dynamically incorporate such prior information could materially reduce the duration and cost of sequential experiments. We could further broaden the impact of our methods by relaxing some of these regularity conditions in future work.

Supplementary Material

These materials include the proofs of Lemma 1, Lemma 2, and Theorem 1, as well as additional content for our examples in Section 5. The code to conduct the numerical studies in the paper is available online: <https://github.com/lmhagar/SeqDesign>.

Funding Acknowledgement

Luke Hagar acknowledges the support of a postdoctoral fellowship from the Natural Sciences and Engineering Research Council of Canada (NSERC). Shirin Golchi acknowledges support from NSERC, Canadian Institute for Statistical Sciences (CANSSI), and Fonds de recherche du Québec - Santé (FRQS).

References

Ashoor, S. H., G. J. Seperich, W. C. Monte, and J. Welty (1983). High performance liquid chromatographic determination of caffeine in decaffeinated coffee, tea, and beverage products. *Journal of the Association of Official Analytical Chemists* 66(3), 606–609.

Berger-Tal, O., J. Nathan, E. Meron, and D. Saltz (2014). The exploration-exploitation dilemma: A multi-disciplinary framework. *PLOS One* 9(4), e95693.

Berry, S. M., B. P. Carlin, J. J. Lee, and P. Muller (2010). *Bayesian adaptive methods for clinical trials*. CRC press.

Bross, I. (1952). Sequential medical plans. *Biometrics* 8(3), 188–205.

De Santis, F. (2007). Using historical data for Bayesian sample size determination. *Journal of the Royal Statistical Society: Series A (Statistics in Society)* 170(1), 95–113.

Demets, D. L. and K. G. Lan (1994). Interim analysis: the alpha spending function approach. *Statistics in Medicine* 13(13-14), 1341–1352.

Deng, A., L. Hagar, N. T. Stevens, T. Xifara, and A. Gandhi (2024). Metric decomposition in A/B tests. In *Proceedings of the 30th ACM SIGKDD Conference on Knowledge Discovery and Data Mining*, pp. 4885–4895.

FDA (2019). Adaptive designs for clinical trials of drugs and biologics — Guidance for industry. Center for Drug Evaluation and Research, U.S. Food and Drug Administration, Rockville, MD.

Gelman, A., X.-L. Meng, and H. Stern (1996). Posterior predictive assessment of model fitness via realized discrepancies. *Statistica sinica*, 733–760.

Golchi, S. (2022). Estimating design operating characteristics in Bayesian adaptive clinical trials. *Canadian Journal of Statistics* 50(2), 417–436.

Golchi, S. and J. J. Willard (2024). Estimating the sampling distribution of posterior decision summaries in Bayesian clinical trials. *Biometrical Journal* 66(8), e70002.

Gubbiotti, S. and F. De Santis (2011). A Bayesian method for the choice of the sample size in equivalence trials. *Australian & New Zealand Journal of Statistics* 53(4), 443–460.

Hagar, L. and N. T. Stevens (2025). An economical approach to design posterior analyses. *Journal of the American Statistical Association*, doi.org/10.1080/01621459.2025.2476221.

Halperin, M., K. G. Lan, J. H. Ware, N. J. Johnson, and D. L. DeMets (1982). An aid to data monitoring in long-term clinical trials. *Controlled Clinical Trials* 3(4), 311–323.

Jenkins, C. and J. Peacock (2011). The power of Bayesian evidence in astronomy. *Monthly Notices of the Royal Astronomical Society* 413(4), 2895–2905.

Jennison, C. and B. W. Turnbull (1999). *Group Sequential Methods with Applications to Clinical Trials*. CRC Press.

Katehakis, M. N. and A. F. Veinott Jr (1987). The multi-armed bandit problem: Decomposition and computation. *Mathematics of Operations Research* 12(2), 262–268.

Klein, M. (2024). Tecovirimat in non-hospitalized patients with monkeypox (platinum-can). <https://clinicaltrials.gov/study/NCT05534165>.

Lachin, J. M. (2005). A review of methods for futility stopping based on conditional power. *Statistics in Medicine* 24(18), 2747–2764.

McCusker, R. R., B. Fuehrlein, B. A. Goldberger, M. S. Gold, and E. J. Cone (2006). Caffeine content of decaffeinated coffee. *Journal of analytical toxicology* 30(8), 611–613.

O'Brien, P. C. and T. R. Fleming (1979). A multiple testing procedure for clinical trials. *Biometrics*, 549–556.

Pocock, S. J. (1977). Group sequential methods in the design and analysis of clinical trials. *Biometrika* 64 (2), 191–199.

Rubin, D. B. (1984). Bayesianly justifiable and relevant frequency calculations for the applied statistician. *The Annals of Statistics*, 1151–1172.

Saville, B. R., J. T. Connor, G. D. Ayers, and J. Alvarez (2014). The utility of Bayesian predictive probabilities for interim monitoring of clinical trials. *Clinical Trials* 11(4), 485–493.

Thompson, W. R. (1933). On the likelihood that one unknown probability exceeds another in view of the evidence of two samples. *Biometrika* 25(3-4), 285–294.

van der Vaart, A. W. (1998). *Asymptotic Statistics*. Cambridge Series in Statistical and Probabilistic Mathematics. Cambridge University Press.

Wald, A. (2004). *Sequential Analysis*. Courier Corporation.

Wang, F. and A. E. Gelfand (2002). A simulation-based approach to Bayesian sample size determination for performance under a given model and for separating models. *Statistical Science* 17(2), 193–208.